Liquid Crystals
Publication details, including instructions for authors and subscription information:
http://www.informaworld.com/smpp/title~content=t713926090

The effect of the polarization electric field on helix-unwinding in a planar chiral smectic C liquid-crystal cell

Tadashi Akahane[a]; Nobuyuki Itoh[a]; Masahiro Nakagawa[a]
[a] Department of Electrical Engineering, Faculty of Engineering, The Technological University of Nagaoka, Niigata, Japan

To cite this Article Akahane, Tadashi , Itoh, Nobuyuki and Nakagawa, Masahiro(1989) 'The effect of the polarization electric field on helix-unwinding in a planar chiral smectic C liquid-crystal cell', Liquid Crystals, 5: 4, 1107 — 1113
To link to this Article: DOI: 10.1080/02678298908026414
URL: http://dx.doi.org/10.1080/02678298908026414

LIQUID CRYSTALS, 1989, VOL. 5, NO. 4, 1107–1113

The effect of the polarization electric field on helix-unwinding in a planar chiral smectic C liquid-crystal cell

by TADASHI AKAHANE, NOBUYUKI ITOH
and MASAHIRO NAKAGAWA

Department of Electrical Engineering, Faculty of Engineering, The Technological University of Nagaoka, Kamitomioka, Nagaoka, Niigata 940-21, Japan

The effect of the polarization electric field on helix-unwinding in a thin planar chiral smectic C liquid-crystal cell is studied by using the nematic-like expression for the elastic deformation free-energy density. It is found that the elongation of the helical pitch when the cell thickness decreases is greater when the spontaneous polarization is larger. This is due to the Coulomb repulsion between polarization charges concentrated at $\pm 2\pi$ disclinations.

1. Introduction

An infinite sample of a chiral smectic C (S_C^*) liquid-crystal phase has a helical structure where the director n, the average molecular orientation, rotates around the helical axis z through an azimuthal angle $\Phi(z) = 2\pi z/p_0$ (p_0 is the inherent helical pitch), keeping a constant tilt Θ with the z axis. In a limited sample, however, the structure is influenced by boundary conditions, and this is reflected in the sample structure. When the helical axis is parallel to the cell substrates, it has been shown experimentally that the pitch increases with decreasing cell thickness, and finally the helix is unwound (i.e. to give surface stabilized ferroelectric liquid crystals).

Glogarova and Pavel have examined this problem theoretically by using continuum theory and showed that three types of structure can exist in planar S_C^* samples, depending on the cell thickness, d [1, 2]. According to their results, the helical configuration is stable when $d > d_{c1}$, the twist non-helical structure when $d_{c1} > d > d_{c2}$, and the uniform state when $d < d_{c2}$. Here d_{c1} and d_{c2} are critical thicknesses.

In an infinite S_C^* sample, free from any boundary effect or external forces, the divergence of the spontaneous polarization $\mathbf{P}_s$ must vanish everywhere through the sample since $\mathbf{P}_s$ lies in the plane of the smectic layer and varies only along the layer normal. In a finite S_C^* sample, however, $\nabla \cdot \mathbf{P}_s$ does not necessarily vanish, and a polarization electric field results [3, 4]. This polarization electric field might affect the stability of each configuration. Here the effect of the polarization electric field on helix-unwinding in thin planar S_C^* samples is investigated by means of a finite-element method. In § 2 the basic equations are given, and these equations are solved by the finite-element method in § 3. Section 4 is devoted to a discussion of the sequence of structural changes in planar S_C^* samples as the cell thickness decreases.

2. Basic equations

The expression for the elastic free-energy density of S_C^* liquid crystals free from any layer undulations has the form

$$f_{\text{elas}} = \tfrac{1}{2}K_1(\nabla \cdot \mathbf{n})^2 + \tfrac{1}{2}K_2(\mathbf{n} \cdot \nabla \times \mathbf{n} + q_\parallel)^2 + \tfrac{1}{2}K_3(\mathbf{n} \times \nabla \times \mathbf{n} + q_\perp \tau)^2, \quad (1)$$

0267-8292/89 $3.00

analogous to the nematic expression [5]. Here K_1, K_2 and K_3 are elastic constants for splay, twist and bend deformations respectively, $q_\parallel$ and $q_\perp$ are the wavenumbers for the inherent twist and bend respectively, and the unit vector $\boldsymbol{\tau}$ is defined by

$$\boldsymbol{\tau} = (\mathbf{n} \times \boldsymbol{\nu})(\mathbf{n} \cdot \boldsymbol{\nu})/|(\mathbf{n} \times \boldsymbol{\nu})(\mathbf{n} \cdot \boldsymbol{\nu})|, \tag{2}$$

where $\boldsymbol{\nu}$ is the layer's unit normal vector. Let the layer normal $\boldsymbol{\nu}$ be along the z axis and the normal to the cell boundary be along the y axis. We assume that the azimuthal angle Φ of the director depends on the y and z coordinates; then

$$\mathbf{n}(y, z) = (\eta \cos\Phi(y, z), \eta \sin\Phi(y, z), \xi), \tag{3}$$

where $\eta = \sin\Theta$ and $\xi = \cos\Theta$. Substituting from equation (3) into equation (1), we obtain

$$\begin{aligned} f_{\text{elas}} = {} & \tfrac{1}{2}(K_1 \cos^2\Phi + K_4 \sin^2\Phi)\eta^2 \left(\frac{\partial\Phi}{\partial y}\right)^2 + \tfrac{1}{2}K_5\eta^2 \left(\frac{\partial\Phi}{\partial z}\right)^2 \\ & + q_1\eta \sin\Phi \left(\frac{\partial\Phi}{\partial y}\right) + q_2\eta \left(\frac{\partial\Phi}{\partial z}\right) + K_6\eta^2 \sin\Phi \left(\frac{\partial\Phi}{\partial y}\right)\left(\frac{\partial\Phi}{\partial z}\right) \\ & + f_0, \end{aligned} \tag{4}$$

where we define

$$\begin{aligned} K_4 &= K_2\xi^2 + K_3\eta^2, \quad K_5 = K_2\eta^2 + K_3\xi^2, \quad K_6 = (K_3 - K_2)\eta\xi, \\ q_1 &= K_2 q_\parallel \xi + K_3 q_\perp \eta, \quad q_2 = -K_2 q_\parallel \eta + K_3 q_\perp \xi, \\ f_0 &= \tfrac{1}{2}K_2 q_\parallel^2 + \tfrac{1}{2}K_3 q_\perp^2. \end{aligned}$$

For an infinite sample, Φ does not depend on y; then, from equation (4), it is easily seen that the helical structure with an intrinsic pitch p_0 given by

$$\left.\begin{aligned} p_0 &= \frac{2\pi}{q_0}, \\ q_0 &= -\frac{q_2}{K_5\eta} \\ &= \frac{K_2 q_\parallel - K_3 q_\perp(\xi/\eta)}{K_2\eta^2 + K_3\xi^2} \end{aligned}\right\} \tag{5}$$

is stable. In the limited sample considered here, however, Φ depends on y in general, and so does the spontaneous polarization vector $\mathbf{P}_s$. Then, $\nabla \cdot \mathbf{P}_s$ does not necessarily vanish, and a polarization electric field results. Therefore we must take account of the interaction energies between the electric field $\mathbf{E}$ and the spontaneous polarization $\mathbf{P}_s$ ($-\mathbf{P}_s \cdot \mathbf{E}$), and the induced polarization ($-\frac{1}{2}\mathbf{D} \cdot \mathbf{E}$) even when there is no external electric field.

Introducing the electric scalar potential $\phi(y, z)$ by

$$\mathbf{E} = -\nabla\phi,$$

the energy density due to the induced polarization is given by

$$\begin{aligned} f_d &= -\tfrac{1}{2}\mathbf{D} \cdot \mathbf{E}, \\ &= \frac{1}{2}\left[\varepsilon_{yy}\left(\frac{\partial\phi}{\partial y}\right)^2 + \varepsilon_{zz}\left(\frac{\partial\phi}{\partial z}\right)^2 + 2\varepsilon_{yz}\left(\frac{\partial\phi}{\partial y}\right)\left(\frac{\partial\phi}{\partial z}\right)\right], \end{aligned} \tag{6}$$

where

$$\varepsilon_{yy} = \varepsilon_4 \sin^2\Phi + \varepsilon_2 \cos^2\Phi,$$
$$\varepsilon_{zz} = \varepsilon_5,$$
$$\varepsilon_{yz} = \Delta\varepsilon\,\eta\xi \sin\Phi,$$
$$\varepsilon_4 = \varepsilon_1\xi^2 + \varepsilon_3\eta^2, \quad \varepsilon_5 = \varepsilon_1\eta^2 + \varepsilon_3\xi^2, \quad \Delta\varepsilon = \varepsilon_3 - \varepsilon_1.$$

Here ε_1, ε_2 and ε_3 are the principal dielectric constants: ε_3 is parallel to the director $\mathbf{n}$, ε_2 is parallel to $\boldsymbol{\tau}$ and ε_1 is parallel to the direction $\mathbf{n} \times \boldsymbol{\tau}$. Finally, the energy density due to the spontaneous polarization is given by

$$\begin{aligned} f_p &= -\mathbf{P}_s \cdot \mathbf{E} \\ &= P_s \cos\Phi \left(\frac{\partial\phi}{\partial y}\right), \end{aligned} \tag{7}$$

where we define $\mathbf{P}_s = -P_s\boldsymbol{\tau}$. The total energy is given by

$$F = \int dy\, dz\, (f_{clas} + f_d + f_p), \tag{8}$$

and this must be minimized under the appropriate boundary conditions. From this condition, we obtain the Euler–Lagrange equations with respect to Φ and ϕ as

$$\begin{aligned} &(K_1 \cos^2\Phi + K_4 \sin^2\Phi)\eta^2 \left(\frac{\partial^2\Phi}{\partial y^2}\right) + K_5\eta^2 \left(\frac{\partial^2\Phi}{\partial z^2}\right) \\ &+ (K_4 - K_1)\eta^2 \sin\Phi\cos\Phi \left(\frac{\partial\Phi}{\partial y}\right)^2 + 2K_6\eta^2 \sin\Phi \left(\frac{\partial^2\Phi}{\partial y\,\partial z}\right) \\ &+ K_6\eta^2 \cos\Phi \left(\frac{\partial\Phi}{\partial y}\right)\left(\frac{\partial\Phi}{\partial z}\right) + (\varepsilon_4 - \varepsilon_2)\sin\Phi\cos\Phi \left(\frac{\partial\Phi}{\partial y}\right)^2 \\ &+ \Delta\varepsilon\,\eta\xi \cos\Phi \left(\frac{\partial\phi}{\partial y}\right)\left(\frac{\partial\phi}{\partial z}\right) + P_s \sin\Phi \left(\frac{\partial\phi}{\partial y}\right) = 0, \end{aligned} \tag{9}$$

$$\begin{aligned} &(\varepsilon_4 \sin^2\Phi + \varepsilon_2 \cos^2\Phi)\left(\frac{\partial^2\phi}{\partial y^2}\right) + \varepsilon_5 \left(\frac{\partial^2\phi}{\partial z^2}\right) - 2\Delta\varepsilon\,\eta\xi \sin\Phi \left(\frac{\partial^2\phi}{\partial y\,\partial z}\right) \\ &+ \Delta\varepsilon\,\eta\xi \cos\Phi \left[\left(\frac{\partial\Phi}{\partial y}\right)\left(\frac{\partial\phi}{\partial y}\right) + \left(\frac{\partial\Phi}{\partial z}\right)\left(\frac{\partial\phi}{\partial z}\right)\right] \\ &+ 2(\varepsilon_4 - \varepsilon_2)\sin\Phi\cos\Phi \left(\frac{\partial\Phi}{\partial y}\right)\left(\frac{\partial\phi}{\partial y}\right) + P_s \sin\Phi \left(\frac{\partial\Phi}{\partial y}\right) = 0. \end{aligned} \tag{10}$$

If we use the one constant approximation ($K_1 = K_2 = K_3 = K$) and neglect the dielectric anisotropy ($\varepsilon_1 = \varepsilon_2 = \varepsilon_3 = \varepsilon$) then equations (9) and (10) reduce to

$$K\eta^2 \left(\frac{\partial^2\Phi}{\partial y^2}\right) + K\eta^2 \left(\frac{\partial\Phi}{\partial z^2}\right) + P_s \sin\Phi \left(\frac{\partial\phi}{\partial y}\right) = 0, \tag{9'}$$

$$\varepsilon \left(\frac{\partial^2\phi}{\partial y^2}\right) + \varepsilon \left(\frac{\partial^2\phi}{\partial z^2}\right) + P_s \sin\Phi \left(\frac{\partial\Phi}{\partial y}\right) = 0. \tag{10'}$$

3. Numerical calculation by the finite-element method

In this study we are mainly concerned with the effects of the polarization electric field, and so we shall neglect the anisotropies of the elastic constants and the dielectric constants. Equations (9′) and (10′) were solved by the finite element method. As there are periodic conditions $\Phi(y, z + p) = \Phi(y, z) + 2\pi$ and $\phi(y, z + p) = \phi(y, z)$, it is sufficient to solve them in the region $0 \leqq y \leqq d$ and $0 \leqq z \leqq p$, where p is the effective pitch. We assume Φ to be fixed at the boundaries (i.e. strong anchoring). Two kinds of boundary condition are considered: one is the homogeneous boundary condition $\Phi(0) = \Phi(d) = 0 \pmod{2\pi}$, and the other is the twist condition $\Phi(0) = \pi \pmod{2\pi}$ and $\Phi(d) = 0 \pmod{2\pi}$. The values of ϕ at the boundaries are taken to be zero. The consistency between the helical structure in the bulk and the unwinding boundary conditions requires the existence of a pair of $\pm 2\pi$ disclinations. The mesh pattern used in the finite-element method is shown in figure 1. The free energy per unit volume (F/pd) is minimized with respect to the positions of the $\pm 2\pi$ disclinations and the effective pitch p. Examples of the director field thus obtained are shown in figure 2. The parameters used in these calculations were tilt angle $\Theta = 20°$, elastic

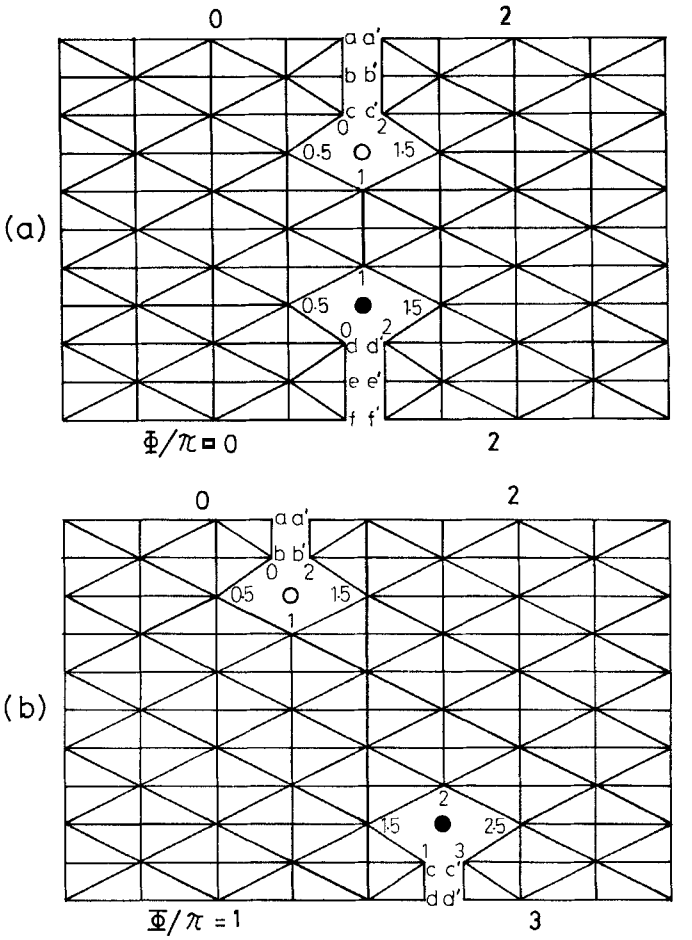

Figure 1. The mesh patterns used in the finite-element method: (*a*) homogeneous boundary condition; (*b*) twist boundary condition. ○ and ● indicate $+2\pi$ and -2π disclinations respectively. a and a′, b and b′, etc. are different nodes but have the same coordinates.

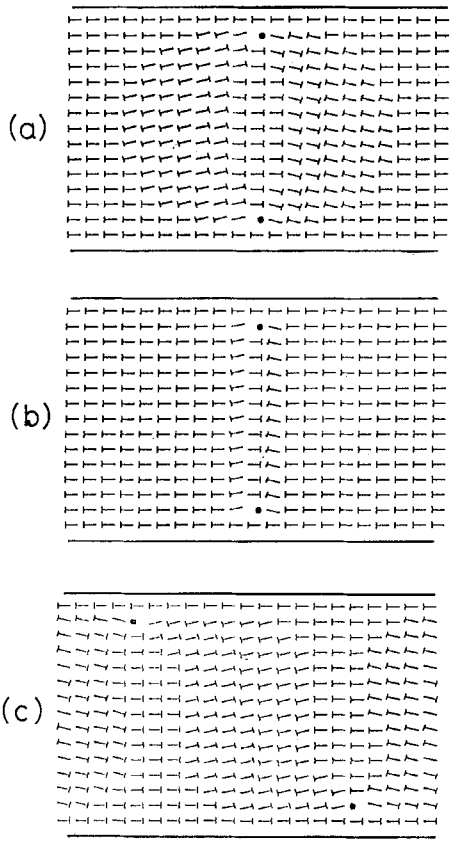

Figure 2. Calculated director fields. (*a*) Homogeneous boundary condition; $d/p_0 = 1{\cdot}0$, $P_s = 2\,\mathrm{nC\,cm^{-2}}$; the effective pitch is calculated to be $p/p_0 = 1{\cdot}2$. (*b*) Homogeneous boundary condition; $d/p_0 = 1{\cdot}0$, $P_s = 10\,\mathrm{nC\,cm^{-2}}$; the effective pitch is $p/p_0 = 4{\cdot}9$. (*c*) Twist boundary condition; $d/p_0 = 1{\cdot}0$, $P_s = 8\,\mathrm{nC\,cm^{-2}}$; the effective pitch is calculated to be $p/p_0 = 1{\cdot}0$.

constant $K = 1{\cdot}0 \times 10^{-11}$ N, dielectric constant $\varepsilon = 5{\cdot}0\varepsilon_0$ (here ε_0 is the electric constant) and the wavenumbers of intrinsic twist and bend $q_{\parallel} = 16{\cdot}6 \times 10^6\,\mathrm{m^{-1}}$, $q_{\perp} = 4.6 \times 10^6\,\mathrm{m^{-1}}$ respectively.

Figure 3 shows the dependence of the effective pitch on the spontaneous polarization. For the homogeneous boundary condition, the effective pitch p increases monotonically as the spontaneous polarization P_s increeases for all values of cell thickness calculated. On the other hand, for the twist boundary condition, p decreases slightly at first and then increases as P_s increases. These results can be interpreted as follows. For the homogeneous boundary condition, we can see from the director field in figures 2 (*a*) and (*b*) that the elastic deformation is limited in the region near the $\pm 2\pi$ disclinations, and this trend increases when P_s becomes large. This means that the polarization charges are sharply concentrated at the disclinations in this case. Owing to Coulomb repulsion between these periodically concentrated polarization charges, it is considered that the effective pitch increases as P_s increases. For the twist boundary condition, however, we can see from figure 2 (*c*) that the elastic deformation is not limited to the region near the disclinations. Consequently, the concentration of the polarization charges is not so marked as for the previous case.

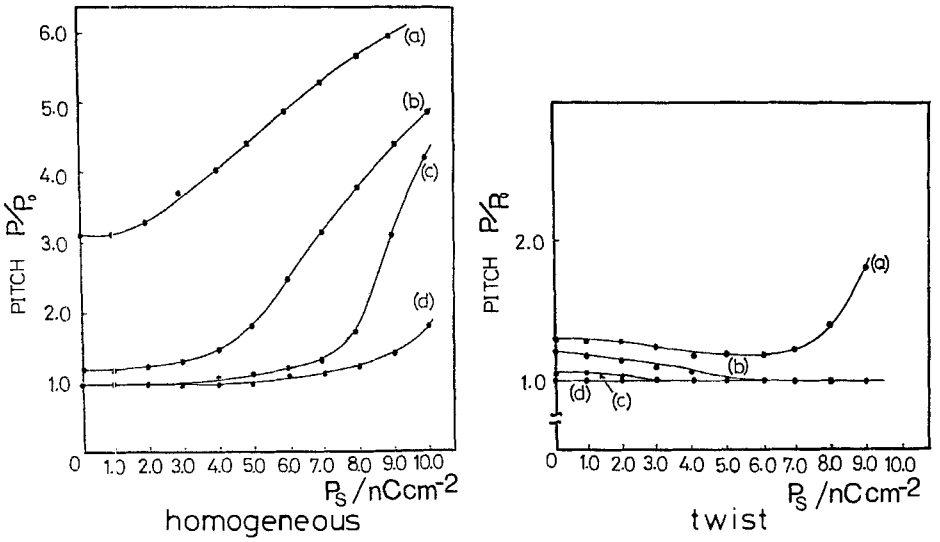

Figure 3. Calculated effective pitch as a function of P_s: (*a*), (*b*), (*c*) and (*d*) are for $d/p_0 = 0{\cdot}7$, 1·0, 1·5 and 2·0 respectively.

4. Discussion

In this section we consider the sequence of structural changes in planar S_C^* samples when the cell thickness decreases and the effect of the polarization electric field on it. We denote the helical structure with the homogeneous boundary condition by H*, the helical one with the twist boundary condition by T*, the unwound non-helical structure with the homogeneous boundary condition by U (the so-called uniform state), and the unwound non-helical structure with the twist boundary condition by T (the so-called twist state).

Figure 4 represents the schematic form of the energy per unit volume of each structure as a function of the cell thickness when the polar anchoring energy at the surface is absent. For the homogeneous boundary condition, H* becomes energetically less

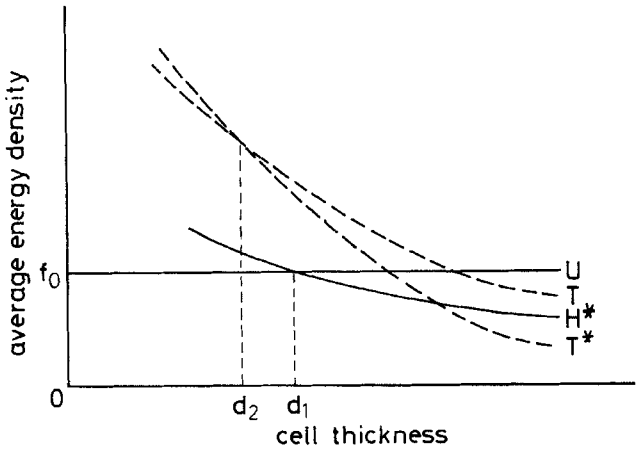

Figure 4. Schematic forms of the energy per unit volume for H*, U, T* and T as functions of the cell thicknesses.

stable than U as the cell thickness decreases below d_1. Similarly, for the twist boundary condition, T* becomes less stable than T as the cell thickness decreases below d_2. Comparing the energies of the homogeneous and the twist boundary conditions, the former is higher than the latter because of the third term on the right-hand side of equation (4) when the cell thickness is large. This term can be transformed into the surface energy and is higher for the homogeneous boundary condition than for the twist boundary condition by the absolute value of $2q_1\eta$. Thus the sequence of structures is considered to be T* → H* → U as the cell thickness decreases.

For real systems, the polar surface anchoring energy must be considered. This polar anchoring energy increases the total energy of H* and U relative to T* and T. Then, as we can see from figure 4, three kinds of structural sequences are possible according to the polar surface anchoring strength: T* → H* → U, T* → U, and T* → T → U. When the spontaneous polarization is larger, the energy density of H* is higher and d_1 increases. In addition to this, the energy densities of T* and T increase more steeply than that of H*. Then the U state is stabilized for thicker cells than for smaller spontaneous polarizations.

References

[1] GLOGAROVA, M., and PAVEL, J., 1984, *J. Phys., Paris*, **45**, 143.
[2] PAVEL, J., 1984, *J. Phys., Paris*, **45**, 137.
[3] NAKAGAWA, M., and AKAHANE, T., 1986, *J. phys. Soc. Japan*, **55**, 1516.
[4] NAKAGAWA, M., and AKAHANE, T., 1986, *J. phys. Soc. Japan*, **55**, 4492.
[5] HANDSCHY, M. A., CLARK, N. A., and LAGERWALL, S. T., 1983, *Phys. Rev. Lett.*, **51**, 471.